

Simultaneous reweighting of Transverse Momentum Dependent distributions

M. Boglione^{a,b}, U. D'Alesio^{c,d}, C. Flore^{a,b,*}, J. O. Gonzalez-Hernandez^{a,b}, F. Murgia^d, A. Prokudin^{e,f}

^aDipartimento di Fisica Teorica, Università di Torino, Via P. Giuria 1, Torino, I-10125, Italy

^bINFN, Sezione di Torino, Via P. Giuria 1, Torino, I-10125, Italy

^cDipartimento di Fisica, Università di Cagliari, Cittadella Universitaria, I-09042 Monserrato (CA), Italy

^dINFN, Sezione di Cagliari, Cittadella Universitaria, I-09042 Monserrato (CA), Italy

^eDivision of Science, Penn State University Berks, Reading, Pennsylvania 19610, USA

^fTheory Center, Jefferson Lab, 12000 Jefferson Avenue, Newport News, Virginia 23606, USA

Abstract

The Bayesian reweighting procedure is extended to the case of multiple independent extractions of transverse momentum dependent parton distributions (TMDs). By exploiting the data on transverse single spin asymmetries, A_N , for inclusive pion production in polarized proton-proton collisions measured at RHIC, we perform a simultaneous reweighting of the quark Sivers, transversity and Collins TMD functions extracted from semi-inclusive deep inelastic scattering (SIDIS) and e^+e^- annihilation into hadron pairs. The impact of the implementation of the Soffer bound, as well as the differences between older and newer A_N data, are investigated. The agreement with A_N data at large- x_F values, a kinematical region complementary to those explored in SIDIS measurements, is enhanced, improving the knowledge of the polarized quark TMDs in the large- x region.

Keywords: Bayesian reweighting, TMDs, Single Spin Asymmetry, Sivers effect, Collins effect

1. Introduction

The idea of incorporating intrinsic transverse motion into the parton distribution functions dates back to the papers by Feynman, Field, and Fox who proposed to use it for the description of the transverse momentum dependent Drell-Yan cross-sections [1, 2]. These functions were later named Transverse Momentum Dependent distribution and fragmentation functions (TMD-PDFs and TMD-FFs), collectively referred to as TMDs, and the TMD formalism was developed for (polarized) Semi-Inclusive Deep Inelastic Scattering (SIDIS), Drell-Yan, and e^+e^- annihilation into hadron pairs [3–10]. QCD factorization theorems were developed for TMDs [11–14] and they were probed experimentally in various processes [15–20]. TMD physics is one of the pillars of the experimental programs of JLab 12 [21] and the future Electron-Ion Collider (EIC) [22, 23], as well as of RHIC [24] at BNL, COMPASS/AMBER [25–27] at CERN, BABAR [19] at SLAC, Belle II [17] at KEK and BESIII [28] in Beijing, of the fixed-target program at the LHC [29] and at Tevatron with the Spin-Quest [30] Drell-Yan program.

Historically, TMDs played a crucial role in explaining spin asymmetries [31–37] and, in particular, the large value of the so-called left-right (A_N) or single-spin asymmetry (SSA) observed in proton-proton collisions [38–54]. Later on, it was

argued that the so-called twist-3 formalism [55, 56] is appropriate for the description of A_N , and it was shown that TMD factorization is, at least formally, violated in hadron production in proton-proton collisions [57]. Nevertheless, TMD and twist-3 formalisms are intimately connected [58], and TMD and twist-3 functions can be related either via specific integral expressions [59–64] or through an operator product expansion [14, 65, 66]. Recently it was demonstrated [67, 68] that spin asymmetries can be successfully fitted using TMD and twist-3 formalisms.

By extending our previous study [69], in this paper we will attempt, for the first time, a simultaneous analysis of the available experimental data for spin asymmetries in SIDIS, e^+e^- scattering, and proton-proton collisions, assuming factorized expressions in terms of TMDs for all those processes. We will exploit two models for the TMD description of A_N : the usual Generalized Parton Model (GPM) [35–37] which assumes that all TMDs are universal, and the Color Gauge Invariant GPM (CGI-GPM) [70–73] that takes into account the process dependence of TMDs due to the direction of gauge links in their corresponding operator definitions. The study will be performed by extending the Bayesian reweighting technique [74–79] to simultaneously reweight the results of new and updated global extractions of the transversity and Sivers distribution functions [80, 81] and of the Collins fragmentation functions (FFs) [82], using presently available data on A_N in proton-proton collisions.

The paper is organized as follows: in Section 2 we recall the TMD formalism, within the GPM and CGI-GPM, while in Section 3 we summarize the basics of the reweighting procedure. A suitable method to treat Monte Carlo sets is discussed in Sec-

*Corresponding author

Email addresses: elena.boglione@to.infn.it (M. Boglione), umberto.dalesio@ca.infn.it (U. D'Alesio), carlo.flore@to.infn.it (C. Flore), joseosvaldo.gonzalezhernandez@unito.it (J. O. Gonzalez-Hernandez), francesco.murgia@ca.infn.it (F. Murgia), prokudin@jlab.org (A. Prokudin)

tion 4. The new independent fits to SIDIS and e^+e^- data are presented in Section 5, while the results of our analysis are discussed in Section 6. Conclusions and final remarks are gathered in Section 7.

2. Formalism

In this Section we summarize the formalism which will guide us throughout our phenomenological analysis.

Starting with the SIDIS processes, $\ell p^\uparrow \rightarrow \ell' h X$, the two azimuthal asymmetries we are interested in are related to the Siverts and the Collins effects, properly defined within a TMD factorization theorem. For the Siverts asymmetry we have [83]

$$A_{UT}^{\sin(\phi_h - \phi_S)} = \frac{F_{UT}^{\sin(\phi_h - \phi_S)}}{F_{UU}}, \quad (1)$$

where $F_{UU} \sim f_1^q \otimes D_1^q$ is the TMD unpolarized structure function, and $F_{UT}^{\sin(\phi_h - \phi_S)} \sim f_{1T}^{\perp q} \otimes D_1^q$ [3, 8, 84] is the azimuthal modulation originating from the correlation between the nucleon spin and the intrinsic transverse momentum of the unpolarized quark. This effect is encoded in the Siverts function.

For the Collins asymmetry, which involves both transversity and Collins functions, one has

$$A_{UT}^{\sin(\phi_h + \phi_S)} = \frac{2(1-y)}{1+(1-y)^2} \frac{F_{UT}^{\sin(\phi_h + \phi_S)}}{F_{UU}}, \quad (2)$$

where y is the fractional energy loss of the incident lepton, and $F_{UT}^{\sin(\phi_h + \phi_S)} \sim h_1^q \otimes H_1^{\perp q}$ [3, 8, 84] is the polarized structure function of the SIDIS cross section, given as a convolution of the TMD transversity distribution, h_1^q , and the Collins FF, $H_1^{\perp q}$. To access this TMD fragmentation function, information from another complementary process, namely $e^+e^- \rightarrow h_1 h_2 X$, is necessary. Here the transverse momentum imbalance of the two hadron, produced in opposite hemispheres, is measured. In this configuration, still within a TMD factorization scheme, a convolution of two Collins FFs appears via a $\cos(2\phi_0)$ modulation [7]:

$$A_0^{ULC} \sim H_1^{\perp \bar{q}} \otimes H_1^{\perp q}. \quad (3)$$

Experimental measurements of this process were conducted at approximately $\sqrt{s} \simeq 10.6$ GeV by the Belle [17] and BABAR [19] collaborations, as well as by the BESIII [28] collaboration, at a lower energy of $\sqrt{s} \simeq 3.65$ GeV.

For inclusive hadron production in pp collisions, the SSA is defined as

$$A_N = \frac{d\sigma^\uparrow - d\sigma^\downarrow}{d\sigma^\uparrow + d\sigma^\downarrow} = \frac{d\Delta\sigma}{2d\sigma}, \quad (4)$$

where $d\sigma^{\uparrow(\downarrow)} \equiv E_h d\sigma^{\uparrow(\downarrow)}/d^3\mathbf{P}_h$ stands for the single-polarized cross section, in which one of the initial-state protons is transversely polarized ($\uparrow(\downarrow)$) with respect to the production plane. Here, we adopt the GPM, a phenomenological model where a factorized formulation in terms of TMDs is assumed as the starting point, and in which one includes spin and transverse momentum correlation effects. For completeness, we will also consider an extension of this approach, the CGI-GPM, where

initial- and final-state interactions are properly included in a one-gluon-exchange approximation. Note that this model allows for the well-known process dependence of the Siverts function expected when comparing SIDIS and Drell-Yan processes [85].

As discussed in Refs. [36, 37], in the region of moderate and forward rapidity in $p^\uparrow p \rightarrow hX$ processes only two effects survive the integration over the intrinsic transverse momenta and their relative azimuthal phases: the Siverts and Collins effects. In the first case, formally, also a contribution from gluons could appear. Nonetheless, in the same kinematical region, the gluon Siverts effect can safely be ignored, as shown in Refs. [73, 86].

It is important to stress that in inclusive processes these two TMD effects cannot be separated. Therefore the numerator of A_N will be

$$d\Delta\sigma \simeq d\Delta\sigma_{\text{Siv}} + d\Delta\sigma_{\text{Col}}. \quad (5)$$

Starting with the Siverts effect, within the CGI-GPM, the numerator of the asymmetry can be schematically written as [70]

$$d\Delta\sigma_{\text{Siv}}^{\text{CGI-GPM}} \propto \sum_{a,b,c,d} f_{1T}^{\perp a}(x_a, k_{\perp a}) \cos\varphi_a \otimes f_{b/p}(x_b, k_{\perp b}) \otimes H_{ab \rightarrow cd}^{\text{Inc}} \otimes D_{h/c}(z, k_{\perp h}), \quad (6)$$

where $f_{b/p}(x_b, k_{\perp b})$ is the TMD distribution for an unpolarized parton b inside the unpolarized proton. Moreover, $H_{ab \rightarrow cd}^{\text{Inc}}$ are the perturbatively calculable hard scattering functions. In particular, the $H_{ab \rightarrow cd}^{\text{Inc}}$ functions where a is a quark or an antiquark can be found in Ref. [70]. The GPM result can be obtained from Eq. (6) by simply replacing $H_{ab \rightarrow cd}^{\text{Inc}}$ with the standard tree-level unpolarized partonic cross sections, $H_{ab \rightarrow cd}^U$. Finally, the unpolarized cross section, $d\sigma$, appearing in the denominator of Eq. (4), can be obtained by replacing the Siverts function and its phase in the GPM expression with the corresponding unpolarized TMD-PDF for parton a .

Focusing now on the Collins contribution, we recall that all FFs (T-even as well as T-odd ones) are process independent, and are not modified by the direction of the gauge links [87, 88]. Thus, the Collins contribution to A_N is assumed to be the same in the GPM and in the CGI-GPM, and reads

$$d\Delta\sigma_{\text{Col}} \propto \sum_{a,b,c,d} h_{1a}(x_a, k_{\perp a}) \otimes f_{b/p}(x_b, k_{\perp b}) \otimes d\Delta\sigma^{a^\uparrow b \rightarrow c^\uparrow d} \otimes H_1^{\perp c}(z, k_{\perp h}), \quad (7)$$

where $d\Delta\sigma^{a^\uparrow b \rightarrow c^\uparrow d} \equiv d\sigma^{a^\uparrow b \rightarrow c^\uparrow d} - d\sigma^{a^\uparrow b \rightarrow c^\downarrow d}$ is the transverse spin transfer at the partonic level.

3. Simultaneous reweighting

We now illustrate the method we have developed for a simultaneous Bayesian reweighting of functions initially extracted from fits to independent datasets. For simplicity, we will focus on the case of *two* functions, although this approach can be easily generalized to n independent extractions.

Let us consider two statistically independent functions, $f(\mathbf{a})$ and $g(\mathbf{b})$ depending, respectively, on n_a - and n_b -dimensional sets of parameters $\mathbf{a} = \{a_1, \dots, a_{n_a}\}$ and $\mathbf{b} = \{b_1, \dots, b_{n_b}\}$. The

value of these parameters is determined by performing two distinct fits to independent datasets \mathbf{E}^a and \mathbf{E}^b . For each of these fits, a χ^2 , defined as ^{1,2}:

$$\begin{aligned}\chi_a^2 &\equiv \chi^2[\mathbf{a}; \mathbf{E}^a] = \sum_{i,j=1}^{N_{\text{dat}}^a} (T_i[\mathbf{a}] - E_i^a) (C_{ij}^a)^{-1} (T_j[\mathbf{a}] - E_j^a), \\ \chi_b^2 &\equiv \chi^2[\mathbf{b}; \mathbf{E}^b] = \sum_{i,j=1}^{N_{\text{dat}}^b} (T_i[\mathbf{b}] - E_i^b) (C_{ij}^b)^{-1} (T_j[\mathbf{b}] - E_j^b),\end{aligned}\quad (8)$$

is minimized and the best fit \mathbf{a}_0 and \mathbf{b}_0 , corresponding to the minima $\chi_{0,a}^2$ and $\chi_{0,b}^2$, are determined. In the equations above, $T_i[\mathbf{a}] \equiv T_i(f(\mathbf{a}))$ are the theoretical estimates corresponding to the experimental data points E_i^a , and C_{ij}^a is the covariance matrix for the fit \mathbf{a} (and similarly for the fit \mathbf{b}). The fit uncertainties can then be computed via a Hessian method or with a suitable Monte Carlo (MC) procedure. Using the latter method, the probability density functions $\pi(\mathbf{a})$ and $\pi(\mathbf{b})$ are reconstructed by generating N_{set}^a sets \mathbf{a}_k and N_{set}^b sets \mathbf{b}_l respectively. Notice that these distributions are statistically independent from each other. Then, expectation values and variances for any quantity \mathcal{O} depending on one of the parameter sets (e.g. \mathbf{a}) can be computed as

$$\begin{aligned}\mathbb{E}[\mathcal{O}] &= \frac{1}{N_{\text{set}}^a} \sum_{k=1}^{N_{\text{set}}^a} \mathcal{O}(\mathbf{a}_k), \\ \mathbb{V}[\mathcal{O}] &= \frac{1}{N_{\text{set}}^a} \sum_{k=1}^{N_{\text{set}}^a} (\mathcal{O}(\mathbf{a}_k) - \mathbb{E}[\mathcal{O}])^2.\end{aligned}\quad (9)$$

Let us now suppose that a new set of data \mathbf{E} (with an associated covariance matrix C) is measured, and that these data can be described by a linear combination of $f(\mathbf{a})$ and $g(\mathbf{b})$ (e.g. $T_i[\mathbf{a}, \mathbf{b}] \equiv \alpha T_i[\mathbf{a}] + \beta T_i[\mathbf{b}]$, where α and β are real constants). Then, we can compute the χ^2 corresponding to these new data as

$$\chi_{\text{new}}^2[\mathbf{a}, \mathbf{b}; \mathbf{E}] = \sum_{i,j=1}^{N_{\text{dat}}} (T_i[\mathbf{a}, \mathbf{b}] - E_i) C_{ij}^{-1} (T_j[\mathbf{a}, \mathbf{b}] - E_j). \quad (10)$$

Since f and g come from statistically independent fits, the uncertainty bands for the theoretical predictions $T_i[\mathbf{a}, \mathbf{b}]$ have to be built by taking all possible ($N_{\text{set}}^a \times N_{\text{set}}^b$) combinations of the MC parameter sets \mathbf{a}_k and \mathbf{b}_l . Thus, the χ^2 on the new data will depend on the k -th and l -th MC sets:

$$\chi_{\text{new}}^2 \equiv \chi_{kl,\text{new}}^2 = \chi_{\text{new}}^2[\mathbf{a}_k, \mathbf{b}_l; \mathbf{E}] \quad (11)$$

leading to ($N_{\text{set}}^a \times N_{\text{set}}^b$) values of χ^2 .

By using Bayes theorem, we can then evaluate the impact of these new data on our prior distributions $\pi(\mathbf{a})$ and $\pi(\mathbf{b})$. Since

¹If (e.g. for the fit \mathbf{a}) only uncorrelated uncertainties σ_i^a are given, the new χ^2 reduces simply to $\chi_a^2[\mathbf{a}; \mathbf{E}^a] = \sum_{i=1}^{N_{\text{dat}}^a} \frac{(T_i[\mathbf{a}] - E_i^a)^2}{(\sigma_i^a)^2}$.

²In what follows the indices (i,j) will be used for individual data points, while the indices (k,l) will refer to MC sets.

these distributions are *a priori* independent, we can build a factorized prior $\pi(\mathbf{a}, \mathbf{b}) = \pi(\mathbf{a})\pi(\mathbf{b})$ and apply Bayes theorem to compute the posterior densities:

$$\mathcal{P}(\mathbf{a}, \mathbf{b}|\mathbf{E}) = \frac{\mathcal{L}(\mathbf{E}|\mathbf{a}, \mathbf{b}) \pi(\mathbf{a}, \mathbf{b})}{Z}, \quad (12)$$

where $\mathcal{L}(\mathbf{E}|\mathbf{a}, \mathbf{b})$ is the likelihood, and $Z = \mathcal{P}(\mathbf{E})$ is the evidence, that ensures a normalized posterior density.

Various choices for the likelihood have been discussed in the literature [74, 75]. Here we adopt the likelihood definition as obtained by taking $\mathcal{L}(\mathbf{E}|\mathbf{a}, \mathbf{b}) d\mathbf{E}$ as the probability to find the new data confined in a differential volume $d\mathbf{E}$ around \mathbf{E} . Following Ref. [89], we define the weights w_{kl} as

$$w_{kl}(\chi_{\text{new}}^2) = \frac{\exp\left\{-\frac{1}{2} \frac{\chi_{kl,\text{new}}^2}{\Delta\chi^2}\right\}}{\sum_{k',l'} \exp\left\{-\frac{1}{2} \frac{\chi_{k'l',\text{new}}^2}{\Delta\chi^2}\right\}}, \quad (13)$$

where $\Delta\chi^2$ is the tolerance at a given confidence level (CL) for $n_a + n_b$ parameters. Notice that the weights coincide with those defined in the original work by Giele and Keller [74], with rescaled exponent: $\chi_{kl}^2 \rightarrow \chi_{kl}^2/\Delta\chi^2$. We will use a value of $\Delta\chi^2$ defined according to Wilks' theorem [90]. For a $(1 - \alpha)$ CL, we have

$$\Delta\chi^2 = F_{\chi_D^2}^{-1}(1 - \alpha), \quad (14)$$

where $F_{\chi_D^2}$ is a chi-squared probability density for D degrees of freedom (i.e. the number of free parameters) and $F_{\chi_D^2}^{-1}$ its associated cumulative function.

The weights are at the core of the reweighting procedure. Using Eq. (13), one can obtain the expectation value and variance of the reweighted quantity \mathcal{O} as

$$\begin{aligned}\mathbb{E}[\mathcal{O}] &= \sum_{k=1}^{N_{\text{set}}^a} \sum_{l=1}^{N_{\text{set}}^b} w_{kl} \mathcal{O}(\mathbf{a}_k, \mathbf{b}_l), \\ \mathbb{V}[\mathcal{O}] &= \sum_{k=1}^{N_{\text{set}}^a} \sum_{l=1}^{N_{\text{set}}^b} w_{kl} (\mathcal{O}(\mathbf{a}_k, \mathbf{b}_l) - \mathbb{E}[\mathcal{O}])^2.\end{aligned}\quad (15)$$

If this quantity depends only on $f(\mathbf{a})$ (or $g(\mathbf{b})$), one has to evaluate the corresponding weights w_k (or w_l)

$$w_k = \sum_{l=1}^{N_{\text{set}}^b} w_{kl}, \quad w_l = \sum_{k=1}^{N_{\text{set}}^a} w_{kl}, \quad (16)$$

and use again the weighted sums in Eq. (15) with the new, updated weights w_k (or w_l) for the corresponding $\mathcal{O}(\mathbf{a}_k)$ (or $\mathcal{O}(\mathbf{b}_l)$). By doing so, one is able to evaluate the impact of the new data on the two independent prior distributions $\pi(\mathbf{a})$ and $\pi(\mathbf{b})$ and on any quantity depending on the parameter sets \mathbf{a} and/or \mathbf{b} . As the weights defined in Eq. (13) are normalized to one, w_k and w_l are automatically normalized to one too.

For a generic extraction with N_{set} MC sets and weights w_k , the rescaled version is equivalent to the Hessian reweighting [89], and allows us to retain a larger effective number of

sets, N_{eff} , defined as

$$N_{\text{eff}} = \exp \left\{ \sum_{k=1}^{N_{\text{set}}} w_k \ln \left(\frac{1}{w_k} \right) \right\}. \quad (17)$$

N_{eff} is related to the number of sets carrying a non-negligible weight, reflecting the method's efficiency. If $N_{\text{eff}} \ll N_{\text{set}}$, the method is considered no longer reliable, signaling that either the new data require a full refitting, or that they are inconsistent with the old ones [75].

In general, the introduction of new data may lead to correlations between fits that were originally statistically independent. For example, this scenario could arise with A_N , which incorporates contributions from both Siverts and Collins effects. Such correlations are encoded in the $(N_{\text{set}}^a \times N_{\text{set}}^b)$ combinations, and are duly considered when evaluating a reweighted quantity.

4. Compressing the MC sets

Following the procedure illustrated in Appendix A of Ref. [91], after the initial fitting stage we generate (*e.g.* for the fit \mathbf{a}) N_{set}^a MC sets \mathbf{a}_k , each with a corresponding $\chi_{a,k}^2 \in [\chi_{0,a}^2, \chi_{0,a}^2 + \Delta\chi_a^2]$. Again, $\chi_{0,a}^2$ is the minimum found by the fit and $\Delta\chi_a^2$ is the tolerance that depends on the number of parameters and is given at a certain CL. These sets allow us to reliably reconstruct the parameter distribution $\pi(\mathbf{a})$, provided a sufficiently large number of sets is generated. For instance, in Refs. [69, 79, 92], the number of sets needed was up to $O(10^6)$. In the case we consider here, involving two independent functions, this implies up to $O(10^{12})$ combinations in Eq. (11). In order to reduce the computational cost, we will use a compression procedure, which we describe in what follows.

Starting from the full sample of parameters \mathbf{a}_k , we select a *random* sample $\mathbf{a}'_k = \{\mathbf{a}'_1, \dots, \mathbf{a}'_{N_{\text{set}}^a}\}$ with $N_{\text{set}}^a \ll N_{\text{set}}^a$. If $\pi(\mathbf{a}'_k) \simeq \pi(\mathbf{a}_k)$, then one also expects that $\pi(O(\mathbf{a}'_k)) \simeq \pi(O(\mathbf{a}_k))$. In other words, if the sample \mathbf{a}'_k renders a statistically equivalent distribution to that of \mathbf{a}_k , the corresponding distributions of any quantity will not differ significantly. Thus, this procedure would help in decreasing the number of combinations to be computed for the simultaneous reweighting.

The question now is how to check that the sampled distribution is statistically equivalent to the full one. As discussed in Section C.2 of Ref. [93], we adopt as an indicator the Welch's t -statistic, defined as

$$t = \frac{\mu_a - \mu_{a'}}{\sqrt{\frac{\sigma_a^2}{N_{\text{set}}^a} + \frac{\sigma_{a'}^2}{N_{\text{set}}^{a'}}}}, \quad (18)$$

which quantifies the difference of the arithmetical means of two samples (in our case, the full sample \mathbf{a}_k and the compressed random sample \mathbf{a}'_k) with unequal variances and sizes. One has to verify that $|t|$ is such that the corresponding p -values are $\gtrsim 0.1$. Provided this condition holds, one can conclude that the sampled distribution and the original distribution are statistically equivalent. Notice that, at variance with Ref. [93], we do not sample in the observable space (*i.e.* A_N in our case), but rather

in the parameter space. Moreover, since the Welch's t -statistic implicitly assumes underlying Gaussian distributions we also verify the compatibility between the medians and *asymmetric* uncertainty intervals of the samples \mathbf{a}'_k and \mathbf{a}_k . This allows us to correctly sample asymmetric distributions. To check how this compression algorithm works, we detail below an explicit example.

4.1. An explicit example

Let us consider the reweighting performed for the quark Siverts function using STAR A_N jet data [69]. Here, we will re-perform the reweighting using the rescaled weights as defined in Eq. (13).

In the original work, $N_{\text{set}}^a = 2 \cdot 10^5$ MC sets were generated and used to represent the uncertainty on the up- and down-quark Siverts functions. Here, we will select a random sample \mathbf{a}'_k of the parameter sets \mathbf{a}_k , with $N_{\text{set}}^{a'} \ll N_{\text{set}}^a$, checking that their corresponding distribution $\pi(\mathbf{a}'_k)$ is statistically equivalent to $\pi(\mathbf{a}_k)$ and re-perform the reweighting using only the reduced sample of sets. By applying the compression algorithm presented above, we select only 1% of the initial sample, *i.e.* $N_{\text{set}}^{a'} = 2 \cdot 10^3$ sets.

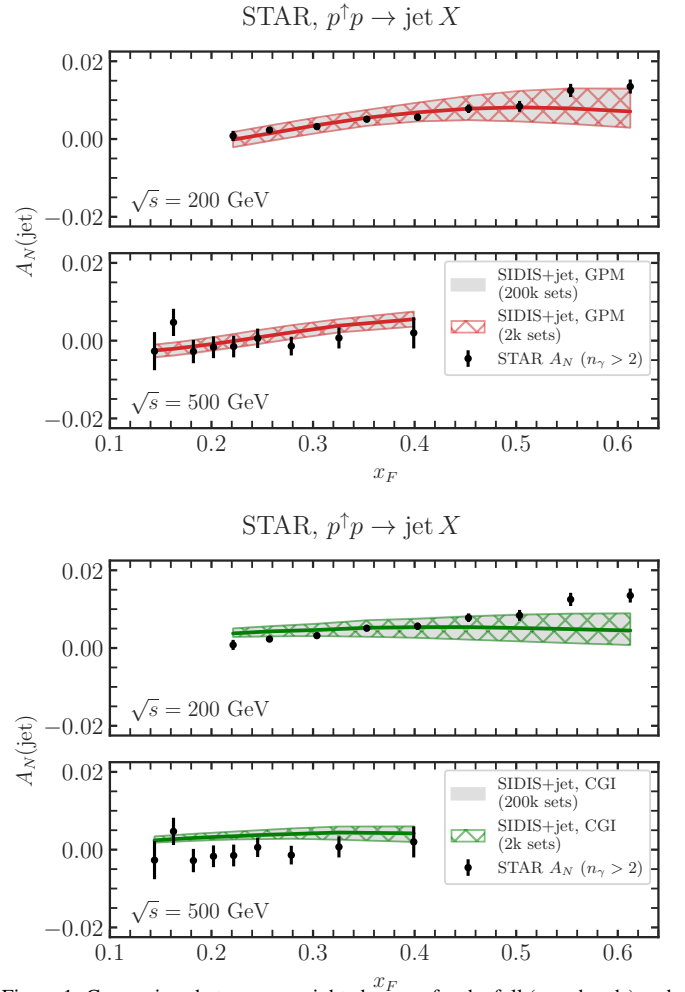


Figure 1: Comparison between reweighted curves for the full (gray bands) and reduced (hatched bands) samples for the reweighting analysis of Ref. [69].

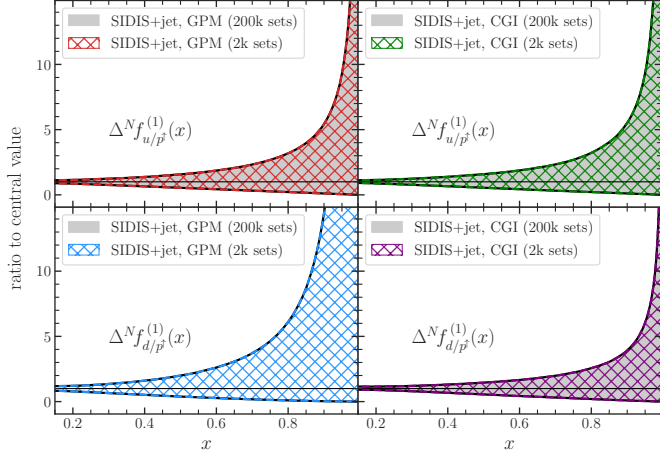


Figure 2: Comparison between reweighted first moments of up- (upper panels) and down-quark (lower panels) Siverson functions, normalized to their central value, using full (gray bands) and reduced (hatched bands) samples for the reweighting analysis of Ref. [69].

Fig. 1 shows the comparison between reweighted curves for the GPM (upper panels) and the CGI-GPM (lower panels), together with STAR data. As in Ref. [69], the central values are the median values, and the asymmetric uncertainty bands are at 2σ CL. The plot clearly shows that median values and uncertainties of the full sample (gray bands) are correctly and satisfactorily reproduced by the reduced sample of MC sets (hatched bands). We verified that the same happens for the unweighted curves, not shown here. For completeness, and to make this comparison more explicit, in Fig. 2 we show the reweighted uncertainties (normalized to their central value) for the Siverson first moment for up- and down-quark in the GPM (left panels) and CGI-GPM (right panels). Reweighted curves from the full sample are shown in gray with black dashed borders, while the ones for the reduced sample are shown in hatched colors. These results allow us to validate the compression procedure, that we will use in what follows for simultaneously reweighting the Siverson, transversity and Collins functions.

5. Priors from SIDIS and e^+e^- data

In this Section we briefly describe the new fits to SIDIS and e^+e^- data for the extraction of the Siverson, transversity and Collins functions. These will represent the priors for the simultaneous reweighting procedure. In all cases we employ updated SIDIS datasets, by including the most recent data from COMPASS [94], HERMES [95] and JLab [20].

The unpolarized TMD PDFs and FFs are parametrized using a factorized Gaussian ansatz:

$$f_{a/p}(x, k_\perp^2) = f_{a/p}(x) \frac{e^{-k_\perp^2/\langle k_\perp^2 \rangle}}{\pi \langle k_\perp^2 \rangle} \quad (19)$$

$$D_{h/q}(z, p_\perp^2) = D_{h/q}(z) \frac{e^{-p_\perp^2/\langle p_\perp^2 \rangle}}{\pi \langle p_\perp^2 \rangle}$$

with $\langle k_\perp^2 \rangle = 0.57 \text{ GeV}^2$ and $\langle p_\perp^2 \rangle = 0.12 \text{ GeV}^2$ as extracted from a fit to HERMES multiplicities [96]. As collinear input,

we adopt the MSHT20nlo proton PDFs [97] and the DEHSS fragmentation functions for pions and kaons [98, 99].

For the up- and down-quark Siverson functions, we adopt the parametrization of Ref. [92], that consists in factorized x and k_\perp dependences (the latter being Gaussian-like and flavor independent):

$$\Delta^N f_{q/p^\dagger}(x, k_\perp) = \frac{4M_p k_\perp}{\langle k_\perp^2 \rangle_S} \Delta^N f_{q/p^\dagger}^{(1)}(x) \frac{e^{-k_\perp^2/\langle k_\perp^2 \rangle_S}}{\pi \langle k_\perp^2 \rangle_S}, \quad (20)$$

where $q = u, d$, M_p is the proton mass, and where $\Delta^N f_{q/p^\dagger}^{(1)}(x)$ is the Siverson first k_\perp -moment [83]:

$$\Delta^N f_{q/p^\dagger}^{(1)}(x) = \int d^2 \mathbf{k}_\perp \frac{k_\perp}{4M_p} \Delta^N f_{q/p^\dagger}(x, k_\perp) \equiv -f_{1T}^{\perp(1)q}(x) \quad (21)$$

$$= N_q (1-x)^{\beta_q}.$$

This model depends on five parameters: N_u , N_d , β_u , β_d , and $\langle k_\perp^2 \rangle_S$.

Following Section 3.1 of Ref. [92], in the computation of F_{UU} (see Eq. (1)), we consistently employ the same collinear PDFs and FFs as for the unpolarized TMDs, and the corresponding Gaussian widths extracted from HERMES and COMPASS multiplicities [96].

For the transversity and Collins functions we make use of the parametrization of Refs. [79, 100]. The transversity function is parametrized as

$$h_1^q(x, k_\perp^2) = h_1^q(x) \frac{e^{-k_\perp^2/\langle k_\perp^2 \rangle}}{\pi \langle k_\perp^2 \rangle}, \quad (22)$$

where the Gaussian width is assumed to be the same as for the unpolarized TMD-PDFs. As in Refs. [79, 100–102], the x -dependent part of the TMD transversity is parametrized at the initial scale Q_0^2 in terms of the Soffer bound [103]:

$$h_1^q(x, Q_0^2) = N_q^T(x) \frac{1}{2} [f_{q/p}(x, Q_0^2) + g_{1L}^q(x, Q_0^2)] \quad (23)$$

$$\equiv N_q^T(x) \text{SB}(x, Q_0^2),$$

where

$$N_q^T(x) = N_q^T x^\alpha (1-x)^\beta \frac{(\alpha + \beta)^{\alpha + \beta}}{\alpha^\alpha \beta^\beta}, \quad (q = u_v, d_v) \quad (24)$$

with the same α and β parameters for the valence u_v and d_v transversity functions, for a total of four parameters for h_1^q . We emphasize that we do not enforce the automatic fulfillment of the Soffer bound ($|N_q^T| \leq 1$), but we apply such a constraint *a posteriori* on the generated MC sets. As shown in Ref. [79], this choice allows us to avoid a bias in the fitting procedure and to properly estimate the uncertainty on the transversity functions.

The Collins function is parametrized as in Refs. [79, 100–102]:

$$H_1^{\perp q}(z, p_\perp^2) = N_q^C(z) \frac{z m_h}{M_C} \sqrt{2e} e^{-p_\perp^2/M_C^2} D_{h/q}(z, p_\perp^2), \quad (25)$$

where $q = \text{fav, unf}$ (favored/unfavored), m_h is the produced hadron mass, and where M_C is a free parameter with mass dimension. $D_{h/q}(z, p_\perp^2)$ is again the unpolarized TMD fragmentation function, while the $N_q^C(z)$ factors are given by

$$N_{\text{fav}}^C(z) = N_{\text{fav}}^C z^\gamma, \quad N_{\text{unf}}^C(z) = N_{\text{unf}}^C, \quad (26)$$

for a total of eight free parameters for the h_1^q and $H_1^{\perp q}$ extraction.

To build the Soffer bound, we adopt the DSSV set [104] for the collinear helicity distributions, $g_{1L}(x)$. By using an appropriately modified version [105, 106] of the HOPPET code [107], a transversity DGLAP kernel is employed to evolve $h_1(x)$ up to higher values of Q^2 . We set $Q_0^2 = 0.81 \text{ GeV}^2$ as the input scale in Eq. (22), with $\alpha_S(M_Z) \simeq 0.118$.

For the collinear part of the Collins function, we also adopt a DGLAP evolution. In principle scale evolution should be taken into account in a more rigorous way. In this case, in particular, the appropriate formalism would be that of TMD factorization leading to TMD evolution equations. There is, however, a general consensus based on experimental evidences that scale evolution effects appear to be mild when it comes to azimuthal or single-spin asymmetries. In fact, asymmetries are defined as *ratios* of cross sections, where evolution and higher order effects tend to cancel out [108]. Although our parametrization does not incorporate the complete features of TMD evolution, phenomenological results based on DGLAP evolution are compatible with full TMD evolution at higher logarithmic accuracy [108, 109] (see also Fig. 14 of Ref. [110]) in the kinematic region we are interested in.

Note that the updated extractions turn out to be compatible with those of Refs. [79, 92, 96], although the new HERMES data induce slightly larger TMD distributions, as already observed in Ref. [68]. For the two independent extractions of TMDs from the Sivers and Collins asymmetries we generate $O(10^5)$ sets using a Markov chain MC that employs a Metropolis-Hastings algorithm with an auto-regressive generating density [111]), and apply the compression algorithm discussed in Section 4 to select $2 \cdot 10^3$ MC sets for each extraction. This amounts to $4 \cdot 10^6$ combinations to be computed for each of the A_N bins for the simultaneous reweighting.

As mentioned above, these updated analyses will represent the priors of the reweighting procedure, which will be described in the following Section.

6. Results

6.1. Simultaneous reweighting with A_N data for inclusive pion production

We start by illustrating the comparison between our predictions for the A_N asymmetry in inclusive production of charged and neutral pions in the GPM and CGI-GPM with the experimental data used for the simultaneous reweighting. We consider as new evidence the preliminary data for A_N measured by BRAHMS for π^\pm production at $\sqrt{s} = 200 \text{ GeV}$ [45], the data from STAR for π^0 production at $\sqrt{s} = 200 \text{ GeV}$ [43, 46, 49] and the latest STAR data for non-isolated π^0 production from Ref. [54] at $\sqrt{s} = 200 \text{ GeV}$ and $\sqrt{s} = 500 \text{ GeV}$.

In our computation of A_N , the transverse momentum of the final state pion, P_T , is the hard scale of the process. For the (CGI-)GPM to be applicable, we then select only data points with $P_T > 1 \text{ GeV}$.

In what follows we adopt the median as central value, and the uncertainties are estimated by determining 2σ -confidence regions. Since we have a total of 13 free parameters (5 for f_{1T}^\perp , 4 for h_1 and 4 for H_1^\perp), according to Eq. (14), we get $\Delta\chi^2 = 22.69$ entering Eq. (13).

Hereafter, we present the unweighted predictions, based on the information from SIDIS and e^+e^- asymmetries only, in gray. The reweighted curves in the GPM and the CGI-GPM are shown respectively with red and green bands. Data points corresponding to $P_T < 1.5 \text{ GeV}$ are depicted in gray, to highlight the kinematic regions where the perturbative approach may be questioned, especially as far as scale uncertainties are concerned (see *e.g.* Ref. [112] for a recent discussion on this issue).

Let us start from the results for charged pion production at BRAHMS. Before entering into our main discussion, few comments are in order. While it is well known that π^0 data are mostly sensitive to the relative contribution of up- and down-quark TMD distributions (Sivers or transversity, depending on the effect considered), π^\pm data allow for a more direct flavor separation, giving a larger discriminating power to any phenomenological study. Therefore, in view of their relevance, we have included the charged pion datasets in our analysis, although yet unpublished and covering a limited kinematical range. Charged pion A_N measurements at future facilities, like the EIC [22, 23], the JLab 22 program [113], AMBER [27] and the proposed fixed-target program at the LHC [29], will indeed help in improving future TMD analyses.

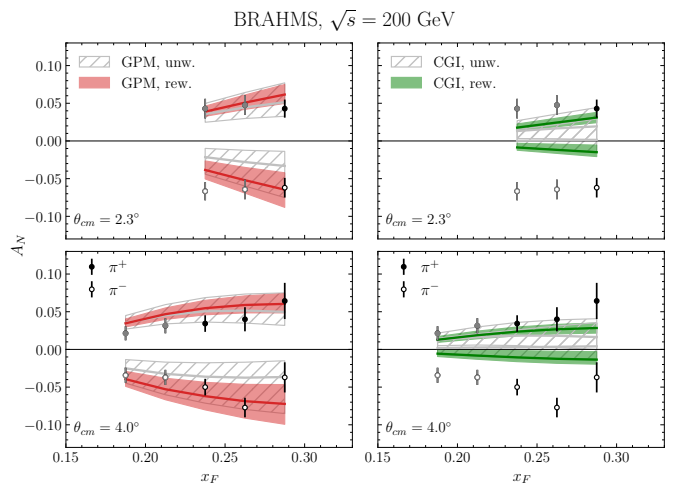


Figure 3: Results for the simultaneous reweighting of the Sivers, transversity and Collins functions: unweighted and reweighted predictions for BRAHMS $A_N^{\pi^\pm}$ data [45] in the GPM (left panels) and the CGI-GPM (right panels) are presented. Data points in gray correspond to $P_T < 1.5 \text{ GeV}$.

In Fig. 3 we show the unweighted and reweighted bands in the GPM and the CGI-GPM, compared to A_N data from BRAHMS for π^+ (full bullet points) and π^- (empty bullet

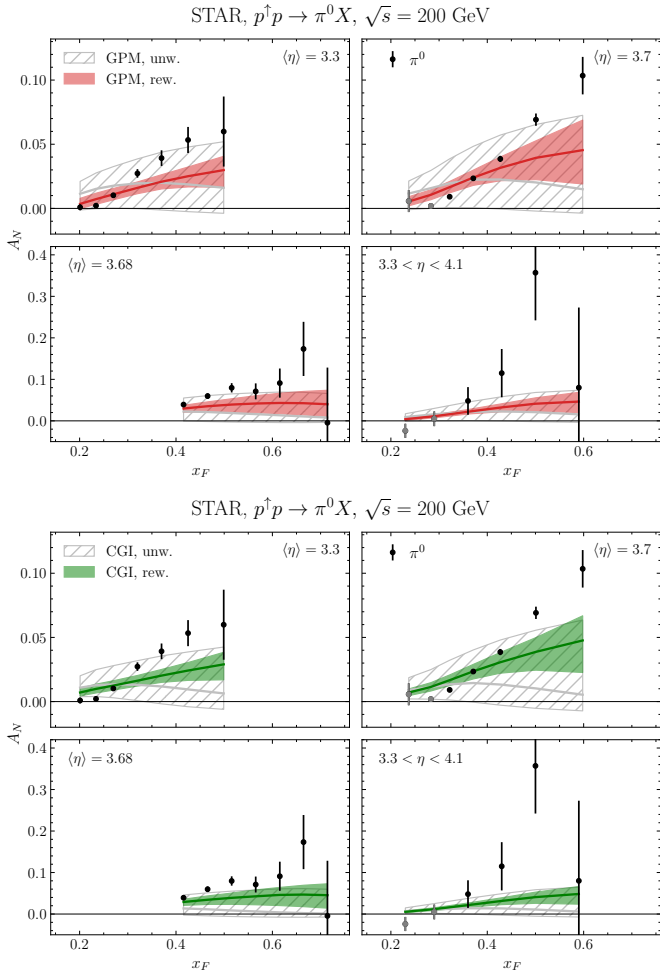


Figure 4: Results for the simultaneous reweighting of the Siverson, transversity and Collins functions: reweighted curves for STAR data [43, 46, 49] in the GPM (upper panels) and the CGI-GPM (lower panels) are presented. Data points in gray correspond to $P_T < 1.5$ GeV.

points). As expected, the reweighted curves present reduced uncertainties. The GPM describes these data better than the CGI-GPM, and the quality of the description increases if one does not consider the aforementioned data points with $P_T < 1.5$ GeV. A somehow larger discrepancy between our computation and the data is seen for π^- in the CGI-GPM.

The comparison with the older STAR data [43, 46, 49], collected without separating isolated and non-isolated pion samples, is shown in Fig. 4 for the GPM (upper panels) and the CGI-GPM (lower panels), in four different ranges of pseudorapidity. Notice that, in the two kinematical configurations with largest $\langle \eta \rangle$ (right plots in the two panels), the first two data points at lower x_F values correspond to $P_T < 1.5$ GeV. Both GPM and CGI-GPM estimates are in qualitative agreement with the data. The reweighted bands are able to describe the data at moderate x_F , and more interestingly, they present a shape that better represents the steady increase of the asymmetry at large- x_F values, where the agreement is enhanced with respect to older analyses [114, 115].

We finally move to the latest STAR data [54] for non-isolated

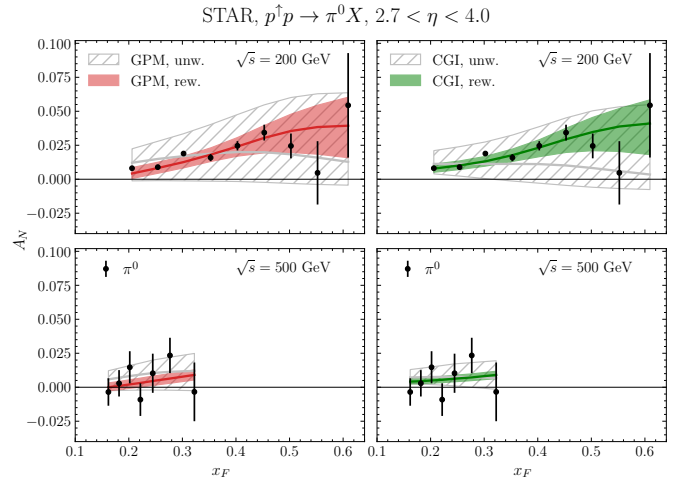


Figure 5: Results for the simultaneous reweighting of the Siverson, transversity and Collins functions: unweighted and reweighted predictions of STAR A_N data for non isolated neutral pions [54]. Comparisons of the asymmetries computed in the GPM (left panels) and in the CGI-GPM (right panels) with experimental data at $\sqrt{s} = 200$ GeV (upper panels) and $\sqrt{s} = 500$ GeV (lower panels) are presented. Here all data points correspond to $P_T > 1.5$ GeV.

π^0 s. The kinematics of this dataset aligns more closely to that of our initial fits in SIDIS and e^+e^- , as it mainly involves pions with moderate momentum fractions z , excluding those with $z \sim 1$ [54]. Furthermore, the A_N data for non-isolated π^0 differ from the corresponding overall π^0 inclusive data sample, and from older A_N measurements in similar kinematical regions [43, 46, 49], as they do not show the usual pronounced steady increase at large x_F (see also Figs. 6, 7 and 8 of Ref. [54] for a more exhaustive comparison). We will present the outcomes of the reweighting procedure, specifically addressing this STAR π^0 dataset, at the end of Section 6.2 (omitting figures for brevity).

In Fig. 5 we show our estimates and compare them against STAR results for non-isolated pions. Both GPM and CGI-GPM describe the data rather well within uncertainties at the two different energies of 200 and 500 GeV. As the reweighting includes information from all the aforementioned datasets, we observe a steady increase at large x_F . However, when the reweighting is limited to the new STAR data alone, the shape of the reweighted bands appears flatter, mirroring the trend of the non-isolated pion data. In Section 6.2, we will also discuss the uncertainties affecting the TMDs and the corresponding N_{eff} obtained from reweighting in this specific case.

6.2. Impact of A_N data on Siverson, transversity and Collins functions

We now examine the role played by A_N data in the extraction of the Siverson, transversity and Collins functions. As a general feature, we anticipate that these data impact mostly on the TMD-PDFs, namely the Siverson and the transversity functions.

We start by examining the Siverson case. In Fig. 6 we compare the unweighted and reweighted first moment of the quark Siverson functions, Eq.(21), in the GPM (left panels) and CGI-GPM (right panels). As a general trend, the reweighted curves present

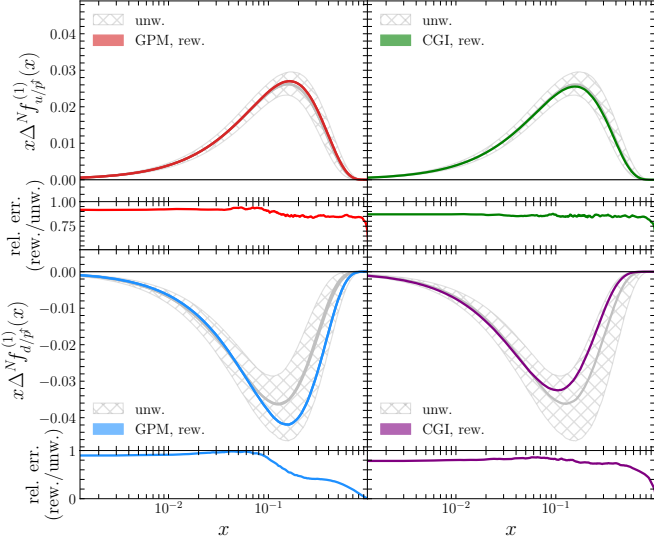


Figure 6: Comparison of unweighted and reweighted first moments of up- (upper panels) and down-quark (lower panels) Sivers functions in the GPM (left panels) and in the CGI-GPM (right panels). The relative reduction of uncertainty is shown in the bottom panels.

reduced uncertainties. This reduction is more pronounced for the d -quark than for the u -quark Sivers function. The relative reduction of uncertainty of the reweighted Sivers first moments is about 20 – 30% for $f_{1T}^{\perp u}$ and 40 – 90% for $f_{1T}^{\perp d}$. The effective number of sets (see Eq. (17)) surviving after reweighting is $N_{\text{eff}} = 547$ (706) in the GPM (CGI-GPM) case. Fig. 7 shows that, in both approaches, the parameters for the u -quark Sivers function and the Gaussian Sivers width do not change much, while the GPM appears to favor a smaller overall absolute value of the normalization for the d -quark Sivers function, with a slower decrease at large x (smaller β_d parameter), while the CGI seem to prefer a larger N_d (in size), but with a faster decrease at large x .

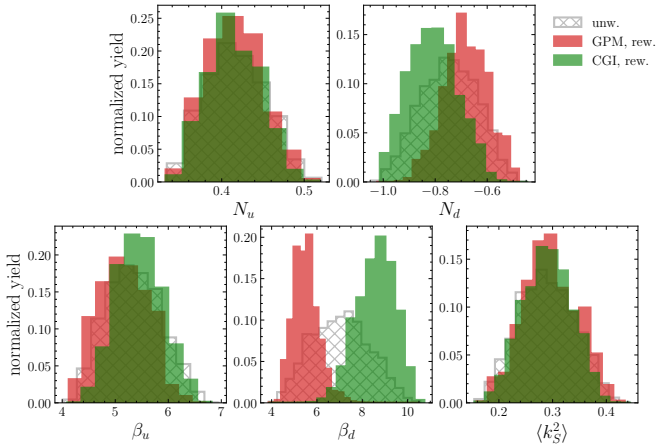


Figure 7: Comparison of unweighted (gray) and reweighted distributions of parameters for the quark Sivers functions in the GPM (red) and in the CGI-GPM (green).

Considering the transversity and Collins case, we empha-

size that, though the Collins contribution to A_N is formally the same in the GPM and CGI-GPM, the results for the reweighted curves for h_1^q and $H_1^{\perp q}$ are slightly different. This reflects the different role of the Sivers contribution to A_N in the two approaches.

In Fig. 8 we present the comparison between unweighted and reweighted u_v and d_v transversity functions, along with their corresponding Soffer bound, in the GPM (left panels) and CGI-GPM (right panels) at $Q^2 = 4 \text{ GeV}^2$. Note that, compared to the unweighted results, A_N data favor on average a slightly smaller $h_1^{u_v}$ in the region $x \lesssim 0.3$ and a slightly larger $h_1^{u_v}$ in the large- x region. The inclusion of A_N data sizeably reduces the uncertainty band in the region of $x \gtrsim 0.3$. As for $h_1^{d_v}$, we observe that a larger absolute value is preferred by the data on A_N . This is induced by the $A_N^{\pi^0}$ data at large x_F (which are related to large x values of the functions probed upon integration), that tend to favor sets yielding large asymmetries. The uncertainty reduction is about 20 – 30% at smaller values of x , extending up to 80 – 90% at larger x values for $h_1^{u_v}$, both in the GPM and in the CGI-GPM, while for $h_1^{d_v}$ the reduction is 30 – 40% (60%) in the GPM (CGI-GPM) at small x and up to 80 – 90% at large x in both cases. Here, the effective number of sets after the reweighting is $N_{\text{eff}} = 285$ (GPM) and $N_{\text{eff}} = 110$ (CGI-GPM). This might be due to the poor description of π^- data (see Fig. 3).

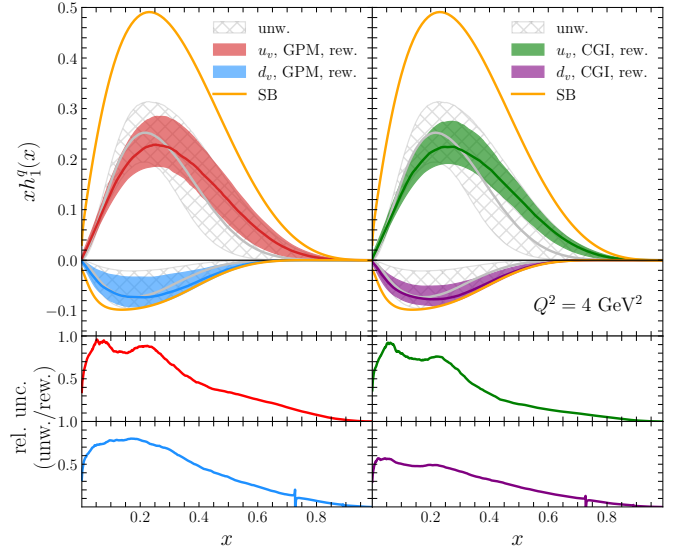


Figure 8: Comparison of unweighted and reweighted u_v and d_v transversity functions in the GPM (left panels) and in the CGI-GPM (right panels). The corresponding Soffer bounds and the relative reduction of uncertainty (same color coding in the bottom panels) are also shown.

In Fig. 9 we show the unweighted and reweighted Collins first moments in the two approaches, at $Q^2 = 4 \text{ GeV}^2$, a typical SIDIS scale. This quantity is defined as [116]

$$\begin{aligned}
 H_1^{\perp(1)q}(z) &= z^2 \int d^2 p_{\perp} \frac{p_{\perp}^2}{2m_h^2} H_1^{\perp q}(z, z^2 p_{\perp}^2) \\
 &= \sqrt{\frac{e}{2}} \frac{1}{2m_h} \frac{M_C^3 \langle p_{\perp}^2 \rangle}{(\langle p_{\perp}^2 \rangle + M_C^2)^2} N_q^C(z) D_{h/q}(z),
 \end{aligned} \tag{27}$$

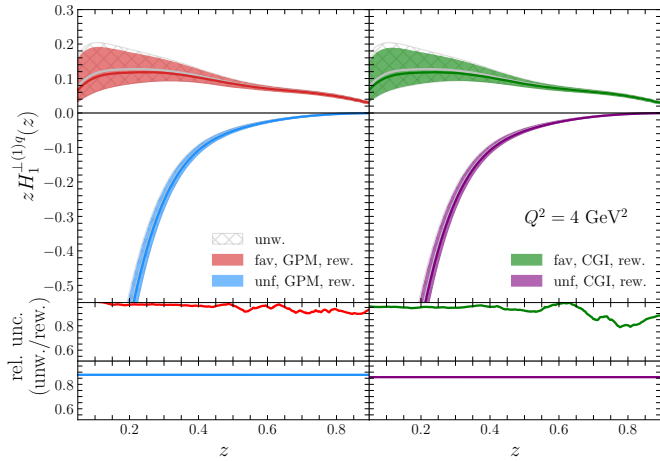


Figure 9: Comparison of unweighted and reweighted favored (upper panels) and unfavored (lower panels) first moments of the Collins functions in the GPM (left panels) and in the CGI-GPM (right panels) at $Q^2 = 4 \text{ GeV}^2$. The relative reduction of uncertainties is shown in the bottom plots.

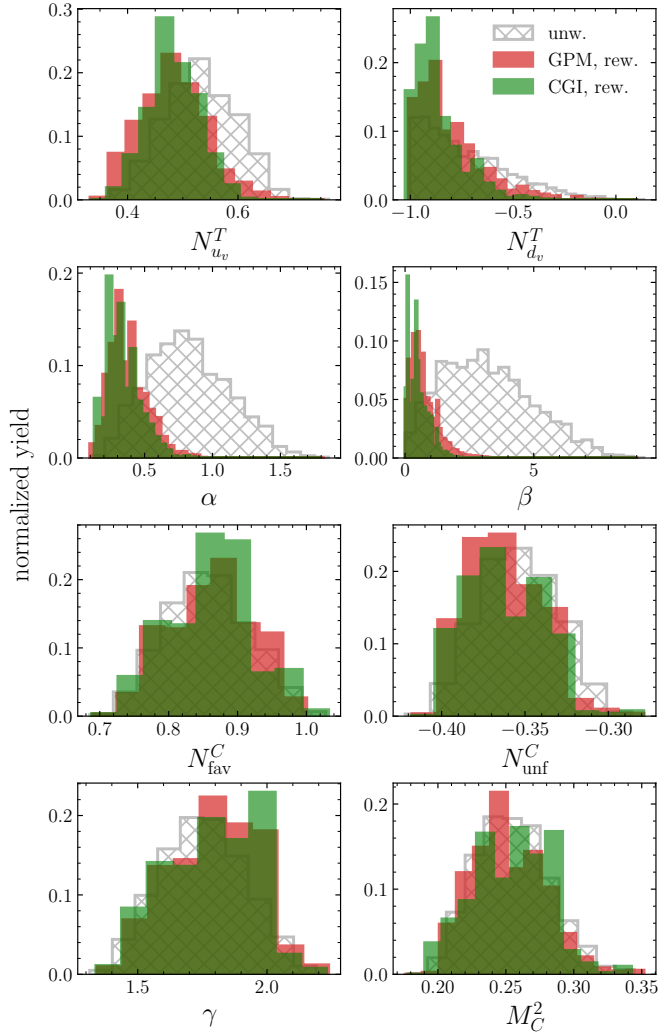


Figure 10: Comparison of unweighted (gray) and reweighted distributions of parameters for the transversity and Collins extraction in the GPM (red) and in the CGI-GPM (green).

where the last line is obtained adopting the parametrization in Eq. (25). For these functions, the impact of A_N data is less strong, but it allows for a reduction of the uncertainties (in both approaches) of about 5-10% for the favored Collins function and about 15% for the unfavored.

The previously mentioned slower decrease of the transversity function for increasing values of x becomes evident when examining Fig. 10, which compares unweighted (hatched gray histograms) and reweighted distributions of the fit parameters in both the GPM (red histograms) and CGI-GPM (green histograms). As noted above, A_N data mainly affect the transversity function. This is clearly represented in the four top panels of Fig. 10: reweighted values of $N_{u_v}^T$ tend to be smaller while the negative $N_{d_v}^T$ values are larger in size, approaching the limiting value of the Soffer bound ($|N_q^T| \leq 1$). At large x , h_1^q tends to decrease following the Soffer bound rather closely (see the corresponding histogram of the β parameter distribution, where the reweighted average values move close to zero). On the other hand, although the Collins parameter distributions show less sizeable variations, the uncertainties of the reweighted Collins functions are still slightly reduced. These considerations point towards the observation that the dominant contribution to A_N is given by the Collins effect. This is consistent with some recent results obtained within the twist-3 approach [67, 68], where it was found that the main contribution to A_N comes from the fragmentation mechanism.

Let us now briefly revisit the induced correlations that emerge from the simultaneous reweighting. We verified that the correlation matrix for the unweighted parameters factorizes into two submatrices (one for the f_{1T}^{\perp} and one for the h_1^q and $H_1^{\perp q}$ parameters). Conversely, as expected, some correlations are introduced by the reweighting procedure, as mentioned in our discussion on simultaneous reweighting. Specifically, we observe weak correlations between the Sivers and transversity normalizations and the β parameters, both within the GPM and the CGI-GPM.

We finally provide a few remarks on the results we obtained for the reweighting procedure using solely the new STAR data for non-isolated π^0 s. Interestingly, we note a more modest reduction in uncertainties of the reweighted TMDs, particularly for the Sivers and Collins functions, while for h_1^q at higher x values the reduction is more sizeable. Furthermore, we observe a higher effective number of retained sets, specifically $N_{\text{eff}} = 1807$ (1961) for the Sivers fit within GPM (CGI-GPM), and $N_{\text{eff}} = 1877$ and 1514 for the transversity and Collins extractions within the GPM and CGI-GPM, respectively. These results appear to suggest a better compatibility between these latest STAR data and measurements from SIDIS and e^+e^- experiments.

6.3. Tensor charges

We conclude our analysis by reporting the corresponding values obtained for the nucleon tensor charges, defined as:

$$\delta q = \int_0^1 [h_1^q(x) - h_1^{\bar{q}}(x)] dx, \quad g_T = \delta u - \delta d. \quad (28)$$

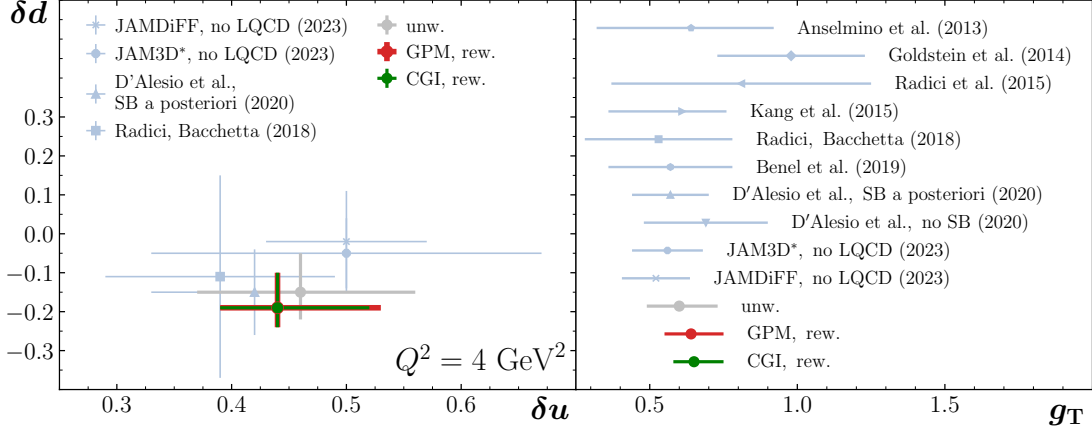


Figure 11: Comparison of our results for the u and d tensor charges (left panel) and the iso-vector combination g_T (right panel) with phenomenological estimates from Refs. [79, 102, 117–122] at $Q^2 = 4 \text{ GeV}^2$. CGI-GPM (green) and GPM (red) reweighted central values almost coincide, having also similar uncertainties.

The values obtained for the *unweighted* transversity functions at $Q^2 = 4 \text{ GeV}^2$ are (central values are the median values): $\delta u = 0.46^{+0.10}_{-0.09}$, $\delta d = -0.15^{+0.10}_{-0.07}$, $g_T = 0.60^{+0.13}_{-0.11}$. The *reweighted* tensor charges in the GPM (CGI-GPM) are: $\delta u = 0.47^{+0.09}_{-0.07}$ ($0.47^{+0.08}_{-0.05}$), $\delta d = -0.18^{+0.10}_{-0.06}$ ($-0.19^{+0.07}_{-0.05}$), $g_T = 0.64^{+0.11}_{-0.09}$ ($0.65^{+0.10}_{-0.07}$). These values are slightly larger as compared to older analyses (see Table 1 of Ref. [79], “using SB” case), due to the new HERMES data on proton, which render larger asymmetries and hence larger fitted functions, as previously observed, for instance, in Ref. [68].

A detailed comparison of our results and various estimates of the tensor charges from phenomenological analyses is presented in Fig. 11. We note that our current analysis and the majority of the previous studies of Refs. [79, 102, 117–122] yield consistent values for g_T , δu , and δd . This corroborates the consistency of different extractions of transversity within different approaches exploiting a variety of experimental data.

7. Conclusions and outlook

In this paper we have investigated the Bayesian reweighting procedure, extending it to the case of multiple, independent fits. For the first time, we have employed this technique to simultaneously reweight two independent extractions of quark TMD parton densities. Specifically, we have focused on the Siverson function and the TMD transversity and Collins functions. To this aim we have considered transverse single spin asymmetries data for inclusive pion production in polarized pp collisions at RHIC.

The simultaneous reweighting involves two statistically independent fits, each with a substantially large MC sample ($O(10^5)$ sets) reflecting their corresponding uncertainty. Since these fits contribute additively to A_N , computing all possible combinations of both MC sets would in principle be necessary. However, to expedite the numerical computation and make them more efficient, we have developed and extended a compression technique for MC set samples. This innovative approach enabled us to exploit only 1% of the sets in the reweighting pro-

cess, without sacrificing any statistical information on parameter distributions. Such optimization not only enhances computational efficiency but also offers enough flexibility for further application to studies involving large sample parameter distributions.

Our phenomenological study, due to its peculiarities, has required an educated selection of the experimental data to be used for the reweighting procedure. The latest A_N^0 data from STAR Collaboration differ from previous measurements at RHIC, as they are provided separating non-isolated from isolated pions. The non-isolated dataset turned out to be more compatible with SIDIS and e^+e^- measurements, for which TMD factorization holds and from which we extract the TMDs, *i.e.* our priors. Note however that, in our comprehensive analysis, we have included *all* available A_N data for charged and neutral pions, obtaining a satisfactory global description.

The adopted dataset is dominated by π^0 production data, while only a few data points from BRAHMS for charged pions are available. As $A_N^{\pi^\pm}$ data are more sensitive to flavor separation, they could help in disentangling the issue of the predicted Siverson sign change. The description of these data seems to favor the GPM, where all TMDs are assumed to be universal and in which, contrary to the CGI-GPM, the expected Siverson sign change is not naturally recovered. The inclusion of data from future experiments, like COMPASS/AMBER [25–27], JLab [21], the EIC [22, 23] and the fixed-target programs at Tevatron at SpinQuest [30], and the LHC [29] would indeed be crucial in shedding light on this fundamental issue.

Our estimates exhibit improved agreement with data compared to previous analyses, owing partly to the careful incorporation of the Soffer bound in the TMD transversity distribution fit. This theoretical constraint, applied *a posteriori*, renders larger asymmetries at large x_F , thereby favoring the dominance of the Collins mechanism, as observed in recent analyses within the collinear twist-3 formalism [67, 68].

Consistently with our previous work [69], the reweighted TMD distributions present reduced uncertainties at large x , confirming once again the complementarity of A_N data with SIDIS

measurements. The reduction in uncertainty is about 40% (90%) for the u -(d -)quark Sivers function, and about 80% to 90% for the u_v and d_v TMD transversity functions. The uncertainty reduction for the Collins functions is smaller (about 10% for the favored and 20% for the unfavored Collins TMDs), confirming that e^+e^- data provide the strongest constraints on this polarized TMD fragmentation function.

By performing the reweighting solely on non-isolated pion data, the reduction in uncertainties is smaller for the Sivers and Collins functions, and similar for the TMD transversity at large x . The retained N_{eff} sets in the GPM (CGI-GPM) case is $\sim 90\%$ ($\sim 95\%$) for the Sivers fit and $\sim 90\%$ ($\sim 75\%$) for the transversity and Collins extraction. This confirms an enhanced compatibility of SIDIS and e^+e^- data with the new A_N measurements from STAR for non-isolated pions.

This work is a natural extension of our previous study [69], and a proof of concept for upcoming TMD analyses. Future studies will explore different TMD parametrizations and incorporate new data from COMPASS/AMBER [26], JLab [21], and from the future Electron-Ion Collider [22, 23]. Additionally, planned investigations into inclusive jet or pion-in-jet production data in pp collisions, where Sivers and Collins effects can be accessed individually, will further contribute to a more comprehensive understanding of TMD dynamics, universality and factorization breaking effects.

Acknowledgments

We thank Mauro Anselmino for numerous discussions. We are grateful to Emanuele Nocera and Andrea Signori for discussions on the statistical approaches and technical aspects of the current analysis. C.F. and A.P. are grateful to the Physics Department of the University of Cagliari and the INFN Cagliari division for the kind hospitality extended to them during the development of this project. A.P. acknowledges financial support from the University of Cagliari under the Visiting Professor Programme. U.D. also acknowledges financial support from Fondazione di Sardegna under the project ‘‘Matter-antimatter asymmetry and polarisation in strange hadrons at LHCb’’, project number F73C22001150007 (University of Cagliari). This article is part of a project that has received funding from the European Union’s Horizon 2020 research and innovation programme under grant agreement STRONG-2020 - No. 824093. This work was partially supported by the Grant for Internationalization SIGA_GFI_22_01 financed by Torino University, by the National Science Foundation under Grants No. PHY-2012002, No. PHY-2310031, No. PHY-2335114 (A.P.), and by the U.S. Department of Energy contract No. DE-AC05-06OR23177, under which Jefferson Science Associates, LLC operates Jefferson Lab (A.P.).

References

[1] R. P. Feynman, R. D. Field, G. C. Fox, Correlations Among Particles and Jets Produced with Large Transverse Momenta, Nucl. Phys. B 128 (1977) 1–65. doi:10.1016/0550-3213(77)90299-1.

[2] R. P. Feynman, R. D. Field, G. C. Fox, A Quantum Chromodynamic Approach for the Large Transverse Momentum Production of Particles and Jets, Phys. Rev. D 18 (1978) 3320. doi:10.1103/PhysRevD.18.3320.

[3] A. Kotzinian, New quark distributions and semiinclusive electroproduction on the polarized nucleons, Nucl. Phys. B 441 (1995) 234–248. arXiv:hep-ph/9412283, doi:10.1016/0550-3213(95)00098-D.

[4] R. D. Tangerman, P. J. Mulders, Intrinsic transverse momentum and the polarized Drell-Yan process, Phys. Rev. D 51 (1995) 3357–3372. arXiv:hep-ph/9403227, doi:10.1103/PhysRevD.51.3357.

[5] R. D. Tangerman, P. J. Mulders, Probing transverse quark polarization in deep inelastic leptonproduction, Phys. Lett. B 352 (1995) 129–133. arXiv:hep-ph/9501202, doi:10.1016/0370-2693(95)00485-4.

[6] D. Boer, P. J. Mulders, Time reversal odd distribution functions in leptonproduction, Phys. Rev. D 57 (1998) 5780–5786. arXiv:hep-ph/9711485, doi:10.1103/PhysRevD.57.5780.

[7] D. Boer, R. Jakob, P. J. Mulders, Asymmetries in polarized hadron production in e^+e^- annihilation up to order $1/Q$, Nucl. Phys. B 504 (1997) 345–380. arXiv:hep-ph/9702281, doi:10.1016/S0550-3213(97)00456-2.

[8] A. Bacchetta, M. Diehl, K. Goeke, A. Metz, P. J. Mulders, M. Schlegel, Semi-inclusive deep inelastic scattering at small transverse momentum, JHEP 02 (2007) 093. arXiv:hep-ph/0611265, doi:10.1088/1126-6708/2007/02/093.

[9] S. Arnold, A. Metz, M. Schlegel, Dilepton production from polarized hadron hadron collisions, Phys. Rev. D 79 (2009) 034005. arXiv:0809.2262, doi:10.1103/PhysRevD.79.034005.

[10] D. Pitonyak, M. Schlegel, A. Metz, Polarized hadron pair production from electron-positron annihilation, Phys. Rev. D 89 (5) (2014) 054032. arXiv:1310.6240, doi:10.1103/PhysRevD.89.054032.

[11] J. C. Collins, D. E. Soper, Back-To-Back Jets in QCD, Nucl. Phys. B 193 (1981) 381, [Erratum: Nucl.Phys.B 213, 545 (1983)]. doi:10.1016/0550-3213(81)90339-4.

[12] J. C. Collins, D. E. Soper, G. F. Sterman, Transverse Momentum Distribution in Drell-Yan Pair and W and Z Boson Production, Nucl. Phys. B 250 (1985) 199–224. doi:10.1016/0550-3213(85)90479-1.

[13] X.-d. Ji, J.-p. Ma, F. Yuan, QCD factorization for semi-inclusive deep-inelastic scattering at low transverse momentum, Phys. Rev. D 71 (2005) 034005. arXiv:hep-ph/0404183, doi:10.1103/PhysRevD.71.034005.

[14] J. Collins, Foundations of perturbative QCD, Cambridge University Press, 2013.

[15] A. Airapetian, et al., Observation of the Naive-T-odd Sivers Effect in Deep-Inelastic Scattering, Phys. Rev. Lett. 103 (2009) 152002. arXiv:0906.3918, doi:10.1103/PhysRevLett.103.152002.

[16] M. Alekseev, et al., Collins and Sivers asymmetries for pions and kaons in muon-deuteron DIS, Phys. Lett. B 673 (2009) 127–135. arXiv:0802.2160, doi:10.1016/j.physletb.2009.01.060.

[17] R. Seidl, et al., Measurement of Azimuthal Asymmetries in Inclusive Production of Hadron Pairs in e^+e^- Annihilation at $s^{**}(1/2) = 10.58$ -GeV, Phys. Rev. D 78 (2008) 032011, [Erratum: Phys.Rev.D 86, 039905 (2012)]. arXiv:0805.2975, doi:10.1103/PhysRevD.78.032011.

[18] C. Adolph, et al., II – Experimental investigation of transverse spin asymmetries in μ^-p SIDIS processes: Sivers asymmetries, Phys. Lett. B 717 (2012) 383–389. arXiv:1205.5122, doi:10.1016/j.physletb.2012.09.056.

[19] J. P. Lees, et al., Measurement of Collins asymmetries in inclusive production of charged pion pairs in e^+e^- annihilation at BABAR, Phys. Rev. D 90 (5) (2014) 052003. arXiv:1309.5278, doi:10.1103/PhysRevD.90.052003.

[20] X. Qian, et al., Single Spin Asymmetries in Charged Pion Production from Semi-Inclusive Deep Inelastic Scattering on a Transversely Polarized ^3He Target, Phys. Rev. Lett. 107 (2011) 072003. arXiv:1106.0363, doi:10.1103/PhysRevLett.107.072003.

[21] J. Dudek, et al., Physics Opportunities with the 12 GeV Upgrade at Jefferson Lab, Eur. Phys. J. A 48 (2012) 187. arXiv:1208.1244, doi:10.1140/epja/i2012-12187-1.

[22] D. Boer, et al., Gluons and the quark sea at high energies: Distributions, polarization, tomography (8 2011). arXiv:1108.1713.

[23] A. Accardi, et al., Electron Ion Collider: The Next QCD Frontier: Understanding the glue that binds us all, Eur. Phys. J. A 52 (9) (2016) 268.

- [arXiv:1212.1701](#), [doi:10.1140/epja/i2016-16268-9](#).
- [24] E.-C. Aschenauer, et al., The RHIC SPIN Program: Achievements and Future Opportunities (1 2015). [arXiv:1501.01220](#).
- [25] F. Gautheron, et al., COMPASS-II Proposal (5 2010).
- [26] F. Bradamante, The future SIDIS measurement on transversely polarized deuterons by the COMPASS Collaboration, PoS SPIN2018 (2018) 045. [arXiv:1812.07281](#), [doi:10.22323/1.346.0045](#).
- [27] B. Adams, et al., Letter of Intent: A New QCD facility at the M2 beam line of the CERN SPS (COMPASS++/AMBER) (8 2018). [arXiv:1808.00848](#).
- [28] M. Ablikim, et al., Measurement of azimuthal asymmetries in inclusive charged dipion production in e^+e^- annihilations at $\sqrt{s} = 3.65$ GeV, Phys. Rev. Lett. 116 (4) (2016) 042001. [arXiv:1507.06824](#), [doi:10.1103/PhysRevLett.116.042001](#).
- [29] C. A. Aidala, et al., The LHCSpin Project (1 2019). [arXiv:1901.08002](#).
- [30] A. Chen, et al., Probing nucleon's spin structures with polarized Drell-Yan in the Fermilab SpinQuest experiment, PoS SPIN2018 (2019) 164. [arXiv:1901.09994](#), [doi:10.22323/1.346.0164](#).
- [31] M. Anselmino, M. Boglione, F. Murgia, Single spin asymmetry for p (polarized) $p \rightarrow \pi X$ in perturbative QCD, Phys. Lett. B 362 (1995) 164–172. [arXiv:hep-ph/9503290](#), [doi:10.1016/0370-2693\(95\)01168-P](#).
- [32] M. Anselmino, M. Boglione, F. Murgia, Phenomenology of single spin asymmetries in p -polarized $p \rightarrow \pi X$, Phys. Rev. D 60 (1999) 054027. [arXiv:hep-ph/9901442](#), [doi:10.1103/PhysRevD.60.054027](#).
- [33] M. Boglione, E. Leader, Reassessment of the Collins mechanism for single spin asymmetries and the behavior of Delta $d(x)$ at large x , Phys. Rev. D 61 (2000) 114001. [arXiv:hep-ph/9911207](#), [doi:10.1103/PhysRevD.61.114001](#).
- [34] M. Anselmino, M. Boglione, U. D'Alesio, E. Leader, F. Murgia, Accessing Sivers gluon distribution via transverse single spin asymmetries in p (transv. polarized) $p \rightarrow D X$ processes at RHIC, Phys. Rev. D 70 (2004) 074025. [arXiv:hep-ph/0407100](#), [doi:10.1103/PhysRevD.70.074025](#).
- [35] U. D'Alesio, F. Murgia, Parton intrinsic motion in inclusive particle production: Unpolarized cross sections, single spin asymmetries and the Sivers effect, Phys. Rev. D 70 (2004) 074009. [arXiv:hep-ph/0408092](#), [doi:10.1103/PhysRevD.70.074009](#).
- [36] M. Anselmino, M. Boglione, U. D'Alesio, E. Leader, S. Melis, F. Murgia, The general partonic structure for hadronic spin asymmetries, Phys. Rev. D 73 (2006) 014020. [arXiv:hep-ph/0509035](#), [doi:10.1103/PhysRevD.73.014020](#).
- [37] U. D'Alesio, F. Murgia, Azimuthal and Single Spin Asymmetries in Hard Scattering Processes, Prog. Part. Nucl. Phys. 61 (2008) 394. [arXiv:0712.4328](#), [doi:10.1016/j.pnpnp.2008.01.001](#).
- [38] G. Bunce, et al., Lambda0 Hyperon Polarization in Inclusive Production by 300-GeV Protons on Beryllium., Phys. Rev. Lett. 36 (1976) 1113–1116. [doi:10.1103/PhysRevLett.36.1113](#).
- [39] R. D. Klem, J. E. Bowers, H. W. Courant, H. Kagan, M. L. Marshak, E. A. Peterson, K. Ruddick, W. H. Dragoset, J. B. Roberts, Measurement of Asymmetries of Inclusive Pion Production in Proton Proton Interactions at 6-GeV/c and 11.8-GeV/c, Phys. Rev. Lett. 36 (1976) 929–931. [doi:10.1103/PhysRevLett.36.929](#).
- [40] D. L. Adams, et al., Comparison of Spin Asymmetries and Cross Sections in π^0 Production by 200 GeV Polarized Antiprotons and Protons, Phys. Lett. B 261 (1991) 201–206. [doi:10.1016/0370-2693\(91\)91351-U](#).
- [41] K. Krueger, et al., Large analyzing power in inclusive π^+ production at high $x(F)$ with a 22-GeV/c polarized proton beam, Phys. Lett. B 459 (1999) 412–416. [doi:10.1016/S0370-2693\(99\)00677-2](#).
- [42] C. E. Allgower, et al., Measurement of analyzing powers of π^+ and π^- produced on a hydrogen and a carbon target with a 22-GeV/c incident polarized proton beam, Phys. Rev. D 65 (2002) 092008. [doi:10.1103/PhysRevD.65.092008](#).
- [43] J. Adams, et al., Cross-sections and transverse single spin asymmetries in forward neutral pion production from proton collisions at $s^{*(1/2)} = 200$ -GeV, Phys. Rev. Lett. 92 (2004) 171801. [arXiv:hep-ex/0310058](#), [doi:10.1103/PhysRevLett.92.171801](#).
- [44] S. S. Adler, et al., Measurement of transverse single-spin asymmetries for mid-rapidity production of neutral pions and charged hadrons in polarized $p+p$ collisions at $s^{*(1/2)} = 200$ -GeV, Phys. Rev. Lett. 95 (2005) 202001. [arXiv:hep-ex/0507073](#), [doi:10.1103/PhysRevLett.95.202001](#).
- [45] J. H. Lee, F. Videbaek, Single spin asymmetries of identified hadrons in polarized $p + p$ at $s^{*(1/2)} = 62.4$ and 200-GeV, AIP Conf. Proc. 915 (1) (2007) 533–538. [doi:10.1063/1.2750837](#).
- [46] B. I. Abelev, et al., Forward Neutral Pion Transverse Single Spin Asymmetries in $p+p$ Collisions at $s^{*(1/2)} = 200$ -GeV, Phys. Rev. Lett. 101 (2008) 222001. [arXiv:0801.2990](#), [doi:10.1103/PhysRevLett.101.222001](#).
- [47] I. Arsene, et al., Single Transverse Spin Asymmetries of Identified Charged Hadrons in Polarized $p+p$ Collisions at $s^{*(1/2)} = 62.4$ -GeV, Phys. Rev. Lett. 101 (2008) 042001. [arXiv:0801.1078](#), [doi:10.1103/PhysRevLett.101.042001](#).
- [48] L. Adamczyk, et al., Longitudinal and transverse spin asymmetries for inclusive jet production at mid-rapidity in polarized $p + p$ collisions at $\sqrt{s} = 200$ GeV, Phys. Rev. D 86 (2012) 032006. [arXiv:1205.2735](#), [doi:10.1103/PhysRevD.86.032006](#).
- [49] L. Adamczyk, et al., Transverse Single-Spin Asymmetry and Cross-Section for π^0 and η Mesons at Large Feynman- x in Polarized $p + p$ Collisions at $\sqrt{s} = 200$ GeV, Phys. Rev. D 86 (2012) 051101. [arXiv:1205.6826](#), [doi:10.1103/PhysRevD.86.051101](#).
- [50] L. C. Bland, et al., Cross Sections and Transverse Single-Spin Asymmetries in Forward Jet Production from Proton Collisions at $\sqrt{s} = 500$ GeV, Phys. Lett. B 750 (2015) 660–665. [arXiv:1304.1454](#), [doi:10.1016/j.physletb.2015.10.001](#).
- [51] A. Adare, et al., Measurement of transverse-single-spin asymmetries for midrapidity and forward-rapidity production of hadrons in polarized $p+p$ collisions at $\sqrt{s} = 200$ and 62.4 GeV, Phys. Rev. D 90 (1) (2014) 012006. [arXiv:1312.1995](#), [doi:10.1103/PhysRevD.90.012006](#).
- [52] A. Adare, et al., Cross section and transverse single-spin asymmetry of η mesons in $p^1 + p$ collisions at $\sqrt{s} = 200$ GeV at forward rapidity, Phys. Rev. D 90 (7) (2014) 072008. [arXiv:1406.3541](#), [doi:10.1103/PhysRevD.90.072008](#).
- [53] U. A. Acharya, et al., Transverse momentum dependent forward neutron single spin asymmetries in transversely polarized $p + p$ collisions at $\sqrt{s} = 200$ GeV, Phys. Rev. D 103 (3) (2021) 032007. [arXiv:2011.14187](#), [doi:10.1103/PhysRevD.103.032007](#).
- [54] J. Adam, et al., Measurement of transverse single-spin asymmetries of π^0 and electromagnetic jets at forward rapidity in 200 and 500 GeV transversely polarized proton-proton collisions, Phys. Rev. D 103 (9) (2021) 092009. [arXiv:2012.11428](#), [doi:10.1103/PhysRevD.103.092009](#).
- [55] J.-w. Qiu, G. F. Sterman, Single transverse spin asymmetries, Phys. Rev. Lett. 67 (1991) 2264–2267. [doi:10.1103/PhysRevLett.67.2264](#).
- [56] J.-w. Qiu, G. F. Sterman, Single transverse spin asymmetries in hadronic pion production, Phys. Rev. D 59 (1999) 014004. [arXiv:hep-ph/9806356](#), [doi:10.1103/PhysRevD.59.014004](#).
- [57] T. C. Rogers, P. J. Mulders, No Generalized TMD-Factorization in Hadro-Production of High Transverse Momentum Hadrons, Phys. Rev. D 81 (2010) 094006. [arXiv:1001.2977](#), [doi:10.1103/PhysRevD.81.094006](#).
- [58] X. Ji, J.-W. Qiu, W. Vogelsang, F. Yuan, A Unified picture for single transverse-spin asymmetries in hard processes, Phys. Rev. Lett. 97 (2006) 082002. [arXiv:hep-ph/0602239](#), [doi:10.1103/PhysRevLett.97.082002](#).
- [59] D. Boer, P. J. Mulders, F. Pijlman, Universality of T odd effects in single spin and azimuthal asymmetries, Nucl. Phys. B 667 (2003) 201–241. [arXiv:hep-ph/0303034](#), [doi:10.1016/S0550-3213\(03\)00527-3](#).
- [60] L. Gamberg, A. Metz, D. Pitonyak, A. Prokudin, Connections between collinear and transverse-momentum-dependent polarized observables within the Collins–Soper–Sterman formalism, Phys. Lett. B 781 (2018) 443. [arXiv:1712.08116](#), [doi:10.1016/j.physletb.2018.03.024](#).
- [61] J.-W. Qiu, T. C. Rogers, B. Wang, Intrinsic Transverse Momentum and Evolution in Weighted Spin Asymmetries, Phys. Rev. D 101 (2020) 116017. [arXiv:2004.13193](#), [doi:10.1103/PhysRevD.101.116017](#).
- [62] M. A. Ebert, J. K. L. Michel, I. W. Stewart, Z. Sun, Disentangling long and short distances in momentum-space TMDs, JHEP 07 (2022) 129.

- [arXiv:2201.07237](#), [doi:10.1007/JHEP07\(2022\)129](#).
- [63] J. O. Gonzalez-Hernandez, T. Rainaldi, T. C. Rogers, Resolution to the problem of consistent large transverse momentum in TMDs, *Phys. Rev. D* 107 (9) (2023) 094029. [arXiv:2303.04921](#), [doi:10.1103/PhysRevD.107.094029](#).
- [64] O. del Rio, A. Prokudin, I. Scimemi, A. Vladimirov, Transverse Momentum Moments (2 2024). [arXiv:2402.01836](#).
- [65] A. Vladimirov, V. Moos, I. Scimemi, Transverse momentum dependent operator expansion at next-to-leading power, *JHEP* 01 (2022) 110. [arXiv:2109.09771](#), [doi:10.1007/JHEP01\(2022\)110](#).
- [66] F. Rein, S. Rodini, A. Schäfer, A. Vladimirov, Sivers, Boer-Mulders and worm-gear distributions at next-to-leading order, *JHEP* 01 (2023) 116. [arXiv:2209.00962](#), [doi:10.1007/JHEP01\(2023\)116](#).
- [67] J. Cammarota, L. Gamberg, Z.-B. Kang, J. A. Miller, D. Pitonyak, A. Prokudin, T. C. Rogers, N. Sato, Origin of single transverse-spin asymmetries in high-energy collisions, *Phys. Rev. D* 102 (5) (2020) 054002. [arXiv:2002.08384](#), [doi:10.1103/PhysRevD.102.054002](#).
- [68] L. Gamberg, M. Malda, J. A. Miller, D. Pitonyak, A. Prokudin, N. Sato, Updated QCD global analysis of single transverse-spin asymmetries: Extracting H^\perp , and the role of the Soffer bound and lattice QCD, *Phys. Rev. D* 106 (3) (2022) 034014. [arXiv:2205.00999](#), [doi:10.1103/PhysRevD.106.034014](#).
- [69] M. Boglione, U. D'Alesio, C. Flore, J. O. Gonzalez-Hernandez, F. Murgia, A. Prokudin, Reweighting the Sivers function with jet data from STAR, *Phys. Lett. B* 815 (2021) 136135. [arXiv:2101.03955](#), [doi:10.1016/j.physletb.2021.136135](#).
- [70] L. Gamberg, Z.-B. Kang, Process dependent Sivers function and implication for single spin asymmetry in inclusive hadron production, *Phys. Lett. B* 696 (2011) 109. [arXiv:1009.1936](#), [doi:10.1016/j.physletb.2010.11.066](#).
- [71] U. D'Alesio, L. Gamberg, Z.-B. Kang, F. Murgia, C. Pisano, Testing the process dependence of the Sivers function via hadron distributions inside a jet, *Phys. Lett. B* 704 (2011) 637. [arXiv:1108.0827](#), [doi:10.1016/j.physletb.2011.09.067](#).
- [72] U. D'Alesio, F. Murgia, C. Pisano, P. Taelis, Probing the gluon Sivers function in $p^\perp p \rightarrow J/\psi X$ and $p^\perp p \rightarrow DX$, *Phys. Rev. D* 96 (2017) 036011. [arXiv:1705.04169](#), [doi:10.1103/PhysRevD.96.036011](#).
- [73] U. D'Alesio, C. Flore, F. Murgia, C. Pisano, P. Taelis, Unraveling the Gluon Sivers Function in Hadronic Collisions at RHIC, *Phys. Rev. D* 99 (2019) 036013. [arXiv:1811.02970](#), [doi:10.1103/PhysRevD.99.036013](#).
- [74] W. T. Giele, S. Keller, Implications of hadron collider observables on parton distribution function uncertainties, *Phys. Rev. D* 58 (1998) 094023. [arXiv:hep-ph/9803393](#), [doi:10.1103/PhysRevD.58.094023](#).
- [75] R. D. Ball, V. Bertone, F. Cerutti, L. Del Debbio, S. Forte, A. Guffanti, J. I. Latorre, J. Rojo, M. Ubiali, Reweighting NNPDFs: the W lepton asymmetry, *Nucl. Phys. B* 849 (2011) 112, [Erratum: *Nucl. Phys. B* 854, 926–927 (2012), Erratum: *Nucl. Phys. B* 855, 927–928 (2012)]. [arXiv:1012.0836](#), [doi:10.1016/j.nuclphysb.2011.03.017](#).
- [76] N. Sato, J. Owens, H. Prosper, Bayesian Reweighting for Global Fits, *Phys. Rev. D* 89 (2014) 114020. [arXiv:1310.1089](#), [doi:10.1103/PhysRevD.89.114020](#).
- [77] N. Sato, J. J. Ethier, W. Melnitchouk, M. Hirai, S. Kumano, A. Accardi, First Monte Carlo analysis of fragmentation functions from single-inclusive e^+e^- annihilation, *Phys. Rev. D* 94 (2016) 114004. [arXiv:1609.00899](#), [doi:10.1103/PhysRevD.94.114004](#).
- [78] H.-W. Lin, W. Melnitchouk, A. Prokudin, N. Sato, H. Shows, First Monte Carlo Global Analysis of Nucleon Transversity with Lattice QCD Constraints, *Phys. Rev. Lett.* 120 (15) (2018) 152502. [arXiv:1710.09858](#), [doi:10.1103/PhysRevLett.120.152502](#).
- [79] U. D'Alesio, C. Flore, A. Prokudin, Role of the Soffer bound in determination of transversity and the tensor charge, *Phys. Lett. B* 803 (2020) 135347. [arXiv:2001.01573](#), [doi:10.1016/j.physletb.2020.135347](#).
- [80] D. W. Sivers, Single Spin Production Asymmetries from the Hard Scattering of Point-Like Constituents, *Phys. Rev. D* 41 (1990) 83. [doi:10.1103/PhysRevD.41.83](#).
- [81] D. W. Sivers, Hard scattering scaling laws for single spin production asymmetries, *Phys. Rev. D* 43 (1991) 261. [doi:10.1103/PhysRevD.43.261](#).
- [82] J. C. Collins, Fragmentation of transversely polarized quarks probed in transverse momentum distributions, *Nucl. Phys. B* 396 (1993) 161. [arXiv:hep-ph/9208213](#), [doi:10.1016/0550-3213\(93\)90262-N](#).
- [83] A. Bacchetta, U. D'Alesio, M. Diehl, C. Miller, Single-spin asymmetries: The Trento conventions, *Phys. Rev. D* 70 (2004) 117504. [arXiv:hep-ph/0410050](#), [doi:10.1103/PhysRevD.70.117504](#).
- [84] P. J. Mulders, R. D. Tangerman, The Complete tree level result up to order $1/Q$ for polarized deep inelastic leptoproduction, *Nucl. Phys. B* 461 (1996) 197–237, [Erratum: *Nucl. Phys. B* 484, 538 (1997)]. [arXiv:hep-ph/9510301](#), [doi:10.1016/S0550-3213\(96\)00648-7](#), [doi:10.1016/0550-3213\(95\)00632-X](#).
- [85] J. C. Collins, Leading twist single transverse-spin asymmetries: Drell-Yan and deep inelastic scattering, *Phys. Lett. B* 536 (2002) 43. [arXiv:hep-ph/0204004](#), [doi:10.1016/S0370-2693\(02\)01819-1](#).
- [86] U. D'Alesio, F. Murgia, C. Pisano, Towards a first estimate of the gluon Sivers function from A_N data in pp collisions at RHIC, *JHEP* 09 (2015) 119. [arXiv:1506.03078](#), [doi:10.1007/JHEP09\(2015\)119](#).
- [87] J. C. Collins, A. Metz, Universality of soft and collinear factors in hard-scattering factorization, *Phys. Rev. Lett.* 93 (2004) 252001. [arXiv:hep-ph/0408249](#), [doi:10.1103/PhysRevLett.93.252001](#).
- [88] F. Yuan, J. Zhou, Collins Fragmentation and the Single Transverse Spin Asymmetry, *Phys. Rev. Lett.* 103 (2009) 052001. [arXiv:0903.4680](#), [doi:10.1103/PhysRevLett.103.052001](#).
- [89] H. Paukkunen, P. Zurita, PDF reweighting in the Hessian matrix approach, *JHEP* 12 (2014) 100. [arXiv:1402.6623](#), [doi:10.1007/JHEP12\(2014\)100](#).
- [90] S. S. Wilks, The Large-Sample Distribution of the Likelihood Ratio for Testing Composite Hypotheses, *Annals Math. Statist.* 9 (1) (1938) 60–62. [doi:10.1214/aoms/1177732360](#).
- [91] M. Anselmino, M. Boglione, U. D'Alesio, A. Kotzinian, S. Melis, F. Murgia, A. Prokudin, C. Turk, Sivers Effect for Pion and Kaon Production in Semi-Inclusive Deep Inelastic Scattering, *Eur. Phys. J. A* 39 (2009) 89–100. [arXiv:0805.2677](#), [doi:10.1140/epja/i2008-10697-y](#).
- [92] M. Boglione, U. D'Alesio, C. Flore, J. Gonzalez-Hernandez, Assessing signals of TMD physics in SIDIS azimuthal asymmetries and in the extraction of the Sivers function, *JHEP* 07 (2018) 148. [arXiv:1806.10645](#), [doi:10.1007/JHEP07\(2018\)148](#).
- [93] B. Bauer, D. Pitonyak, C. Shay, Numerical study of the twist-3 asymmetry ALT in single-inclusive electron-nucleon and proton-proton collisions, *Phys. Rev. D* 107 (1) (2023) 014013. [arXiv:2210.14334](#), [doi:10.1103/PhysRevD.107.014013](#).
- [94] M. Aghasyan, et al., Transverse-momentum-dependent Multiplicities of Charged Hadrons in Muon-Deuteron Deep Inelastic Scattering, *Phys. Rev. D* 97 (3) (2018) 032006. [arXiv:1709.07374](#), [doi:10.1103/PhysRevD.97.032006](#).
- [95] A. Airapetian, et al., Azimuthal single- and double-spin asymmetries in semi-inclusive deep-inelastic lepton scattering by transversely polarized protons, *JHEP* 12 (2020) 010. [arXiv:2007.07755](#), [doi:10.1007/JHEP12\(2020\)010](#).
- [96] M. Anselmino, M. Boglione, J. Gonzalez Hernandez, S. Melis, A. Prokudin, Unpolarised Transverse Momentum Dependent Distribution and Fragmentation Functions from SIDIS Multiplicities, *JHEP* 04 (2014) 005. [arXiv:1312.6261](#), [doi:10.1007/JHEP04\(2014\)005](#).
- [97] S. Bailey, T. Cridge, L. A. Harland-Lang, A. D. Martin, R. S. Thorne, Parton distributions from LHC, HERA, Tevatron and fixed target data: MSHT20 PDFs, *Eur. Phys. J. C* 81 (4) (2021) 341. [arXiv:2012.04684](#), [doi:10.1140/epjc/s10052-021-09057-0](#).
- [98] D. de Florian, R. Sassot, M. Epele, R. J. Hernández-Pinto, M. Stratmann, Parton-to-Pion Fragmentation Reloaded, *Phys. Rev. D* 91 (1) (2015) 014035. [arXiv:1410.6027](#), [doi:10.1103/PhysRevD.91.014035](#).
- [99] D. de Florian, M. Epele, R. J. Hernandez-Pinto, R. Sassot, M. Stratmann, Parton-to-Kaon Fragmentation Revisited, *Phys. Rev. D* 95 (9) (2017) 094019. [arXiv:1702.06353](#), [doi:10.1103/PhysRevD.95.094019](#).
- [100] M. Anselmino, M. Boglione, U. D'Alesio, J. O. Gonzalez Hernandez, S. Melis, F. Murgia, A. Prokudin, Collins functions for pions from SIDIS and new e^+e^- data: a first glance at their transverse momentum dependence, *Phys. Rev. D* 92 (11) (2015) 114023. [arXiv:1510.05389](#), [doi:10.1103/PhysRevD.92.114023](#).
- [101] M. Anselmino, M. Boglione, U. D'Alesio, A. Kotzinian, F. Murgia,

- A. Prokudin, C. Turk, Transversity and Collins functions from SIDIS and e^+e^- data, Phys. Rev. D75 (2007) 054032. [arXiv:hep-ph/0701006](#), [doi:10.1103/PhysRevD.75.054032](#).
- [102] M. Anselmino, M. Boglione, U. D'Alesio, S. Melis, F. Murgia, A. Prokudin, Simultaneous extraction of transversity and Collins functions from new SIDIS and e^+e^- data, Phys. Rev. D87 (2013) 094019. [arXiv:1303.3822](#), [doi:10.1103/PhysRevD.87.094019](#).
- [103] J. Soffer, Positivity constraints for spin dependent parton distributions, Phys. Rev. Lett. 74 (1995) 1292–1294. [arXiv:hep-ph/9409254](#), [doi:10.1103/PhysRevLett.74.1292](#).
- [104] D. de Florian, R. Sassot, M. Stratmann, W. Vogelsang, Extraction of spin-dependent parton densities and their uncertainties, Phys. Rev. D80 (2009) 034030. [arXiv:0904.3821](#), [doi:10.1103/PhysRevD.80.034030](#).
- [105] A. Courtoy, A. Bacchetta, M. Radici, A. Bianconi, First extraction of Interference Fragmentation Functions from e^+e^- data, Phys. Rev. D85 (2012) 114023. [arXiv:1202.0323](#), [doi:10.1103/PhysRevD.85.114023](#).
- [106] A. Bacchetta, private communication (2015).
- [107] G. P. Salam, J. Rojo, A Higher Order Perturbative Parton Evolution Toolkit (HOPPET), Comput. Phys. Commun. 180 (2009) 120–156. [arXiv:0804.3755](#), [doi:10.1016/j.cpc.2008.08.010](#).
- [108] Z.-B. Kang, A. Prokudin, F. Ringer, F. Yuan, Collins azimuthal asymmetries of hadron production inside jets, Phys. Lett. B 774 (2017) 635. [arXiv:1707.00913](#), [doi:10.1016/j.physletb.2017.10.031](#).
- [109] U. D'Alesio, F. Murgia, C. Pisano, Testing the universality of the Collins function in pion-jet production at RHIC, Phys. Lett. B 773 (2017) 300–306. [arXiv:1707.00914](#), [doi:10.1016/j.physletb.2017.08.023](#).
- [110] L. Adamczyk, et al., Azimuthal transverse single-spin asymmetries of inclusive jets and charged pions within jets from polarized-proton collisions at $\sqrt{s} = 500$ GeV, Phys. Rev. D 97 (3) (2018) 032004. [arXiv:1708.07080](#), [doi:10.1103/PhysRevD.97.032004](#).
- [111] S. Chib, E. Greenberg, Understanding the Metropolis-Hastings Algorithm, The American Statistician 49 (1995) 327. [doi:https://doi.org/10.2307/2684568](#).
- [112] A. Colpani Serri, Y. Feng, C. Flore, J.-P. Lansberg, M. A. Ozelik, H.-S. Shao, Y. Yedelkina, Revisiting NLO QCD corrections to total inclusive J/ψ and Υ photoproduction cross sections in lepton-proton collisions, Phys. Lett. B 835 (2022) 137556. [arXiv:2112.05060](#), [doi:10.1016/j.physletb.2022.137556](#).
- [113] A. Accardi, et al., Strong Interaction Physics at the Luminosity Frontier with 22 GeV Electrons at Jefferson Lab (6 2023). [arXiv:2306.09360](#).
- [114] M. Anselmino, M. Boglione, U. D'Alesio, E. Leader, S. Melis, F. Murgia, A. Prokudin, On the role of Collins effect in the single spin asymmetry A_N in $p^\uparrow p \rightarrow hX$ processes, Phys. Rev. D 86 (2012) 074032. [arXiv:1207.6529](#), [doi:10.1103/PhysRevD.86.074032](#).
- [115] M. Anselmino, M. Boglione, U. D'Alesio, S. Melis, F. Murgia, A. Prokudin, Sivers effect and the single spin asymmetry A_N in $p^\uparrow p \rightarrow hX$ processes, Phys. Rev. D 88 (2013) 054023. [arXiv:1304.7691](#), [doi:10.1103/PhysRevD.88.054023](#).
- [116] S. Meissner, A. Metz, D. Pitonyak, Momentum sum rules for fragmentation functions, Phys. Lett. B690 (2010) 296–303. [arXiv:1002.4393](#), [doi:10.1016/j.physletb.2010.05.037](#).
- [117] G. R. Goldstein, J. O. Gonzalez Hernandez, S. Liuti, Flavor dependence of chiral odd generalized parton distributions and the tensor charge from the analysis of combined π^0 and η exclusive electroproduction data (1 2014). [arXiv:1401.0438](#).
- [118] M. Radici, A. Courtoy, A. Bacchetta, M. Guagnelli, Improved extraction of valence transversity distributions from inclusive dihadron production, JHEP 05 (2015) 123. [arXiv:1503.03495](#), [doi:10.1007/JHEP05\(2015\)123](#).
- [119] Z.-B. Kang, A. Prokudin, P. Sun, F. Yuan, Extraction of Quark Transversity Distribution and Collins Fragmentation Functions with QCD Evolution, Phys. Rev. D93 (1) (2016) 014009. [arXiv:1505.05589](#), [doi:10.1103/PhysRevD.93.014009](#).
- [120] M. Radici, A. Bacchetta, First Extraction of Transversity from a Global Analysis of Electron-Proton and Proton-Proton Data, Phys. Rev. Lett. 120 (19) (2018) 192001. [arXiv:1802.05212](#), [doi:10.1103/PhysRevLett.120.192001](#).
- [121] J. Benel, A. Courtoy, R. Ferro-Hernandez, A constrained fit of the valence transversity distributions from dihadron production, Eur. Phys. J. C 80 (5) (2020) 465. [arXiv:1912.03289](#), [doi:10.1140/epjc/s10052-020-8039-y](#).
- [122] C. Cocuzza, A. Metz, D. Pitonyak, A. Prokudin, N. Sato, R. Seidl, Transversity Distributions and Tensor Charges of the Nucleon: Extraction from Dihadron Production and Their Universal Nature, Phys. Rev. Lett. 132 (9) (2024) 091901. [arXiv:2306.12998](#), [doi:10.1103/PhysRevLett.132.091901](#).